Combustion and Flame 201 (2019) 181–186

Contents lists available at ScienceDirect

Combustion and Flame

journal homepage: www.elsevier.com/locate/combustflame

Comparison study of the ignition and combustion characteristics of directly-written Al/PVDF, Al/Viton and Al/THV composites

Haiyang Wang, Miles Rehwoldt, Dylan J. Kline, Tao Wu, Peng Wang, Michael R. Zachariah*

Department of Chemical and Biomolecular Engineering and Department of Chemistry and Biochemistry, University of Maryland, College Park, MD 20742, United States

ARTICLE INFO

Article history:
Received 26 November 2018
Revised 19 December 2018
Accepted 25 December 2018
Available online 31 December 2018

Keywords:
PVDF
Viton
THV
Fluorine
Polymer

ABSTRACT

The aluminum–fluorine reaction is attracting growing interest due to its higher density over aluminum–oxygen. Fluorine rich polymers are particularly interesting for their applications as an energetic binder in advanced additive manufacturing of energetic materials. In this paper, three soluble polymers of PVDF (59 wt% F), Viton (66 wt% F) and THV (73 wt% F) are incorporated with aluminum nanoparticles (Al NPs) and prepared as free-standing films using solvent-based direct writing. The three composite films are compared for their mechanical properties as well as the ignition and combustion performance. Tensile stress was found to order as Al/PVDF > Al/THV > Al/Viton while the elasticity of Al/Viton is much higher than the other two. The burn rate of different composite films increases with Al content, while the flame temperature peaks slightly fuel-rich. The Al/PVDF had the highest burn rate, however, the flame temperature ordered as Al/THV (~2500 K) > Al/Viton (~2000 K) > Al/PVDF (~1500 K), consistent with fluorine content. With higher fluorine and lower hydrogen content, THV releases more CF_x gas than HF, which generates higher temperature. However, HF which is predominantly produced from PVDF has the lowest ignition by far and may be responsible for its high flame speed.

1. Introduction

The oxidation of aluminum fuel with fluorine is 2× more energy dense than that of aluminum–oxygen on a molar basis, attracting attention as an energetic additive in propellants, explosives, and pyrotechnics [1–3]. Fluorine-rich polymers such as PTFE (polymer of tetrafluoroethylene), PVDF (polymer of vinylidene fluoride), Viton (dipolymers of hexafluoropropylene and vinylidene fluoride), and THV (terpolymers of tetrafluoroethylene, hexafluoropropylene and vinylidene fluoride) stand out for their high fluorine content, low melting point and plasticity [4–10]. These materials can also serve as polymeric binders to provide the mechanical integrity to energetic composites. While PTFE has the highest fluorine content of ~76 wt% it is insoluble in any known solvent, thus limiting its practical application. However, many other fluorocarbons, while having slightly lower fluorine content have found application as oxidative binders. Huang et al. [4] prepared a free-standing Al/PVDF film via an electrospray deposition technique, which showed excellent mechanical properties even with Al nanoparticle content as high as 50 wt%. In addition to the work discussed above, the low melting point of PVDF enabled McCollum and coworkers [11] to extrude Al/PVDF into thin filaments as the feed source to prepare films through 3D-printing. The energy density for Al/PVDF which is roughly estimated as 947.7 kJ per mol of aluminum, while the value for the convectional Al/CuO is only 600 kJ per mol of aluminum [1–5]. Viton was commonly used in Magnesium/Teflon/Viton (MTV) composites, which have been in use since the 1950s as payloads in infrared decoy flare applications [12]. Groven and coworkers [9,13] developed a THV based ink with nano and micro Al which enabled the formation of 3D structures. However, no systematic inter-comparison has been explored between these three fluoropolymers and is the subject of this paper.

Currently, there is enthusiasm for utilizing additive manufacturing strategies to obtain structural energetic materials and a variety of methods have already been explored including templating [14], melting-extruding [11,15], inkjet-printing [16], electrophoretic deposition [17], photopolymerization [18] and electrospray [4]. Among these direct writing is one of the most popular because of its relative simplicity and convenience [9,19–21]. Also, direct writing of energetic materials works with a solvent which is desirable for safety purposes. In this paper, three different fluorine polymers of PVDF, Viton, and THV incorporating Al NPs were prepared by direct writing and were comparatively investigated for their film-forming properties, ignitability, activation

* Corresponding author.
E-mail address: mrz@umd.edu (M.R. Zachariah).

https://doi.org/10.1016/j.combustflame.2018.12.031
0010-2180/

Table 1
Physiochemical properties of the three polymers.

	PVDF	Viton a	THV
Molecule weight	534,000	–	–
Density (g/cm^3)	~1.78	>1.8	1.9-2.0
Melting point (°C)	177	–	–
Fluorine (wt%)	59.4	66	73
Hydrogen (wt%)	3.1	1.9	0.6
Carbon (wt%)	37.5	32.1	26.4

energy, mechanical properties, burn rate, flame temperature, and combustion products. As the data in this study will demonstrate, Al/PVDF has the highest burn rate and mechanical tensile elasticity while Al/THV burns at the highest flame temperature. With the increase of Al content, the burn rates of all the three composite films increase while the flame temperatures peak around a slight fuel rich ratio. Species released from three composite films were detected and the combustion products were also examined to propose a possible mechanism.

2. Experimental section

2.1. Chemicals and precursors

Aluminum nanoparticles (Al NPs, ~85 nm, ~81 wt% active Al) were purchased from Novacentrix. PVDF (Molecule weight: 534,000), Viton® A and THV® were ordered from Sigma-Aldrich, Chemours Company, and 3 M Company, respectively. N, N-Dimethylformamide (DMF, 99.8%) was purchased from BDH chemicals. All chemicals were used as received. As Table 1 lists, PVDF, Viton, and THV have a fluorine content of ~59 wt%, ~66 wt% and ~73 wt%, respectively, according to vendor's description. To prepare an Al/PVDF precursor with an equivalence ratio of 1.0, 500 mg PVDF was completely dissolved in 5 mL DMF, and then 174 mg Al NPs were added into the solution and sonicated for 1 h. After stirring for 24 h, the precursor was ready for direct writing. To prepare an Al/Viton and Al/THV precursor with an equivalence ratio of 1.0, the polymer concentrations remain the same but the added Al NPs are different owing to different fluorine content of the polymers. The stoichiometric Al mass fraction for Al/PVDF, Al/Viton and Al/THV is 25.8 wt%, 27.8 wt% and 30.0 wt%, respectively (phi = 1). The calculations were based on Eq. (1) with the consideration of active aluminum content in Al NPs and fluorine content in each polymer. Composite films (10 layers unless specified otherwise) with different Al content were also prepared, with a fixed polymer concentration and a different mass fraction of Al NPs.

$$\frac{z}{3}\mathrm{Al} + \mathrm{C}_x\mathrm{H}_y\mathrm{F}_z = \frac{z}{3}\mathrm{AlF}_3 + x\mathrm{C} + \frac{y}{2}\mathrm{H}_2 \quad (1)$$

2.2. Direct writing of free-standing films

For film fabrication a Hyrel System 30 M printer was employed with a heating stage. The precursor was loaded in a 30 mL syringe with a feed rate of ~4.5 mL/h (measured feed rate) and a needle size of ~0.7 mm. The stage coupled with a glass substrate was heated to ~80 °C before printing, to enable solvent evaporation prior to printing a subsequent layer. The printed area was 2 cm × 2 cm, printed in 10 layers unless specified otherwise. The samples were peeled off from the glass substrate and then cut into 2 cm × 0.25 cm sections for the following tests.

2.3. SEM, EDS, XRD, TG/DSC/MS, and mechanical property test

The microstructure of Al/PVDF, Al/Viton, and Al/THV films was investigated by using a Hitachi SU-70 scanning electron microscope (SEM) coupled to an energy dispersive spectrometer (EDS). The films were sectioned in liquid nitrogen and attached to a carbon film on an SEM stage. The films were also characterized by a thermogravimetry (TG, TA Instruments Q600) and a mass spectrometer at an argon flow of 100 mL/min and a heating rate of 10 °C/min. The combustion products were characterized by powder X-ray diffraction (XRD, Bruker D8 with Cu K radiation). The tensile strength of the films was measured using a Shimazu Autograph AGS-X tensile tester.

2.4. Burning rate and flame temperature measurement

The films were ignited by a Joule-heated nichrome wire (~1 cm in length, 0.010 in. in diameter) in a ~30 mL quartz tube filled with argon (10 L/min argon flow for 5 min). Film burning was recorded using a high-speed camera at a rate of 7000 pps (Vision Research Phantom Miro M110 high-speed camera). The tests for each sample were conducted in triplicate and the average burning rate with the standard error was reported [3]. To estimate the flame temperature of the burning films, color ratio pyrometry was performed using the same high-speed color camera according to a modified Gray-body assumption and then a fitted Planck's Law and the temperatures raw data were obtained [22]. Only unsaturated pixels above the black level and within the error threshold are used to report the mean temperature of the frame for a contiguous area of at least 10 acceptable pixels.

2.5. T-Jump ignition and time-of-flight mass spectrometry

The details of T-jump time-of-flight mass spectrometry (T-Jump MS) method to determine ignition temperature and the temporal evolution of species can be found in ref. [23]. Typically, a ~10 mm long platinum filament (~76 µm in diameter) is coated with a thin layer of film with a thickness of ~1–2 µm. Then the filament is resistively heated to ~1400 K at a heating rate of $\sim 4 \times 10^5$ K s^{-1} in 1 atm of Argon to achieve ignition. The ignition process and subsequent combustion were monitored using a high-speed camera (14.9 µs exposure with 256 × 256 pixels, Phantom V12.1, 76,000 pps). The ignition temperature was calculated by coupling the observed ignition timestamp from the high-speed video with the wire temperature profile. A high speed, time-of-flight mass spectrometer was also coupled with to the ignition filament in vacuum, which is used for detecting the species released during fast heating.

3. Results

Three composite films of stoichiometric Al/PVDF (Fig. 1a), Al/Viton (Fig. 1b) and Al/THV (Fig. 1c) were prepared by direct writing 10 layers with the same mass of ink and under the same printing conditions. The SEM images with low- and high-resolution as well as the stress–strain curves are shown in Fig. 1. All the films show uniform thickness with sharp edges, which indicates precise flow rate control by the direct writing process. SEM also reveals smooth, void-free films, indicating good solvent evaporation during drying. PVDF and Viton have a similar density of 1.8 g/cm^3, while THV has a higher density (~1.95 g/cm^3), thus Al/THV will has a lower volume if the total mass is fixed. Consequently, the resulting thickness of PVDF- and Viton-films was roughly the same (~160 µm) while the THV was thinner (~130 µm). Considering they are all 10 layers (L), the writing speed for the PVDF- and Viton-composite films is ~16 µm/L, and ~13 µm/L for the THV.

As the high-resolution SEM images show, the morphology of the three composites films is significantly different. Consistent with of our previous studies [3,4,24], Fig. 1a-1 (Al/PVDF) shows a thin PVDF network (honeycomb structure) in which Al NPs are embedded. This structure results in a high tensile strength (~35 MPa)

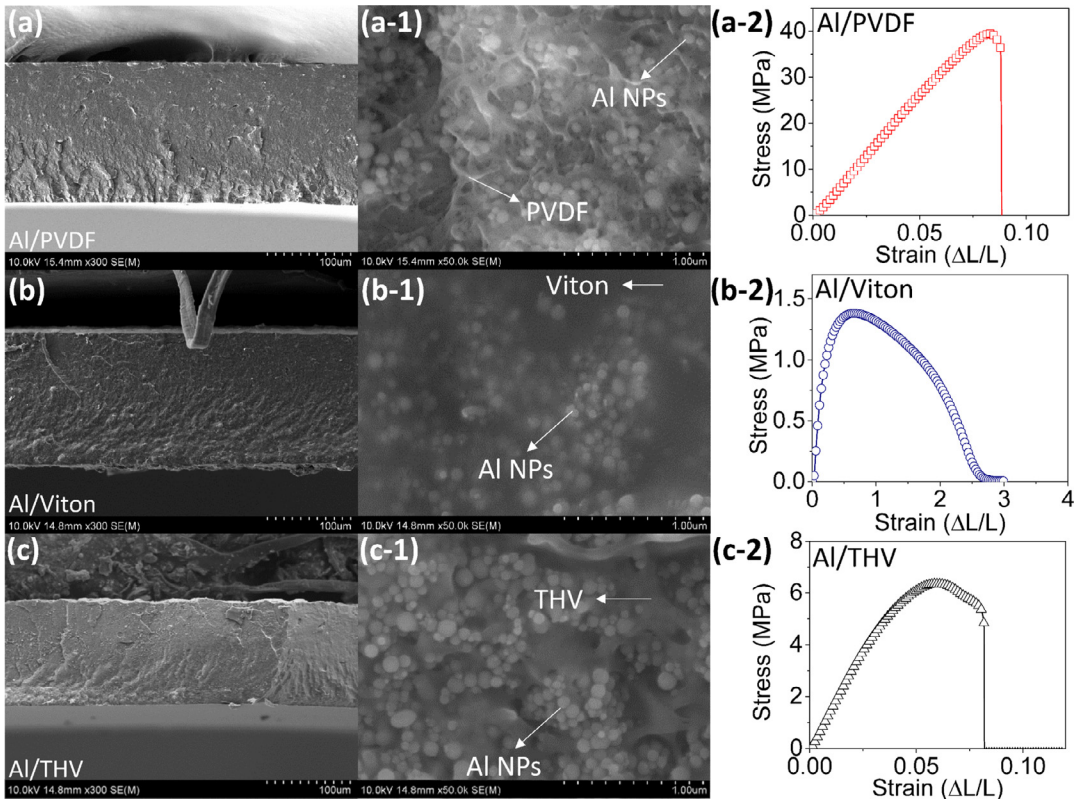

Fig. 1. Low and high resolution SEM images, and stress–strain curves of directly written Al/PVDF (a), Al/Viton (b) and Al/THV (c) films (10 layers). Note different axis in stress–strain diagrams.

with a Young's Modulus of 0.7 GPa. Figure 1c-1 (Al/THV) shows a similar structure, but THV does not form as extensive a network as PVDF resulting in a yield stress of only ~6.5 MPa and a Young's Modulus of ~0.1 GPa. As for the Al/Viton case, no network is seen in SEM (Fig. 1b-1), and Al NPs were encapsulated in the whole Viton matrix. Due to the rubber-like property of Viton, the yield stress is as low as ~1.2 MPa and Young's Modulus is only ~0.002 GPa, which is ~50 and ~350 times lower than that of THV and PVDF, respectively. However, the elasticity of Viton is much higher than the other two, with > 30 times higher strain before fracture.

The fuel-oxidizer ratio is an important parameter which will not only affect the physical properties such as thickness and morphology but also directly manipulate the combustion performance [25]. In this study, composite films with various Al content from ~17 wt% (fuel lean) to 50 wt% (fuel rich) were prepared (SEM were shown in Figs. S1 and S2). The thickness, as well as the burn rate of the films varying with particle loading of Al NPs is shown in Fig. 2a and b, respectively. The thickness of the films increases with the increase of particle loading of Al NPs in the polymer matrix which we speculate to be correlated with two factors. The first factor is that the structure of the films tends to be more porous owing to Al NPs packing more loosely with less binder content available to fill the voided space. The second reason is that, for an ink, higher particle loading results in higher viscosity (less flowability) which results in narrower but thicker lines written by the printer; the latter point is likely to be the reason thickness increased abruptly from 45 wt% to 50 wt% for Al/PVDF 10-layer case. Overall, the thickness increases with particle loading effect (Al/PVDF > Al/Viton > Al/THV) is highly sensitive to the viscosity of the inks (Al/PVDF > Al/Viton > Al/THV) [9,26], which will be discussed in future work and out of the scope of this study.

As Fig. 2b shows, the average linear burn rate (in argon) does not peak at the stoichiometric ratio (26–30 wt% Al) but keeps increasing with the particle loading, most likely due to enhanced gas production and heat convection with more reactive fuel [17,27]. Considering the slope of the curves in Fig. 2b, the burn rate of Al/PVDF increases linearly from 17 wt% to 50 wt% Al while that of Al/Viton and Al/THV are less sensitive to particle loading when fuel content is > 30 wt% (phi = 1). The linear increase in burn rate for the Al/PVDF case may be due to the enhanced pre-ignition effects induced by the Al_2O_3-PVDF reaction as a result of the higher Al_2O_3 mass fraction [1,3,28]. PVDF has the highest hydrogen content and the most likely to release HF (catalyzed by Al_2O_3) to promote the pre-ignition by etching the shell [3,28,29]. However, this argument needs further experimental evidence. It is also noted that the burn rate trend of Al/PVDF case doesn't change with different thickness of either 5 layers or 10 layers, which further confirms the uniform dispersion of Al NPs in different layers and indicates steady combustion of the whole film.

The burn behavior of the different composite films was captured by a high-speed camera with typical snapshots shown in Fig. 3, from which one can see the flame fronts proceed steadily for all the three cases. Besides the slightly different burn rates we mentioned in Fig. 2b, the other differences in the burning for the three films are the flame size and brightness, which are in the order of Al/THV > Al/Viton > Al/PVDF, suggesting that the flame temperatures might follow the same order.

The flame temperatures of the three composites films (with different Al content) were obtained by color ratio pyrometry with a high-speed color camera [22]. The summarized average flame temperature (Fig. 4a), typical snapshot and estimated flame temperature map are shown in Fig. 4b-4d. In summary, the average flame temperatures for stoichiometric Al/PVDF (Fig. 4b), Al/Viton (Fig. 4c) and Al/THV (Fig. 4d) are ~1500 K, ~2000 K, and ~2500 K, respectively. With the increase of Al content, the flame temperature of Al/Viton and Al/THV peaks slight fuel-rich but is less sensitive in Al/PVDF.

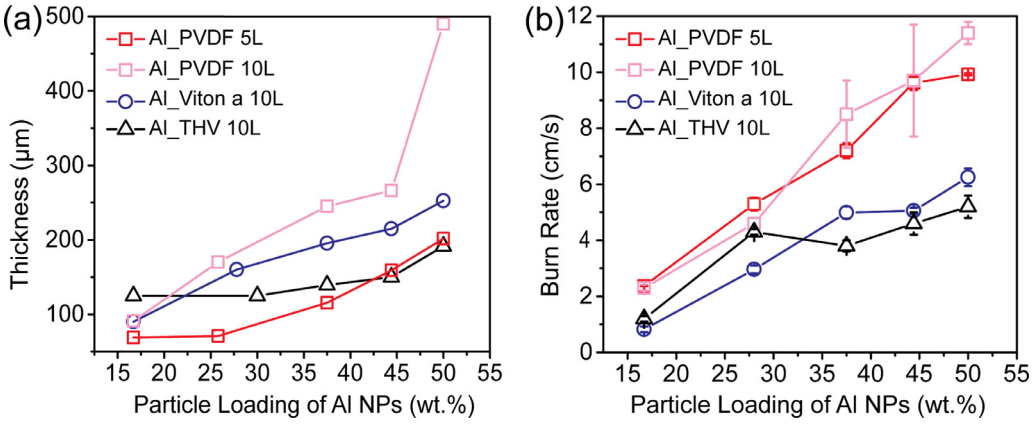

Fig. 2. The thickness (a) and burn rate (b) of different films changing with the particle loading of Al NPs.

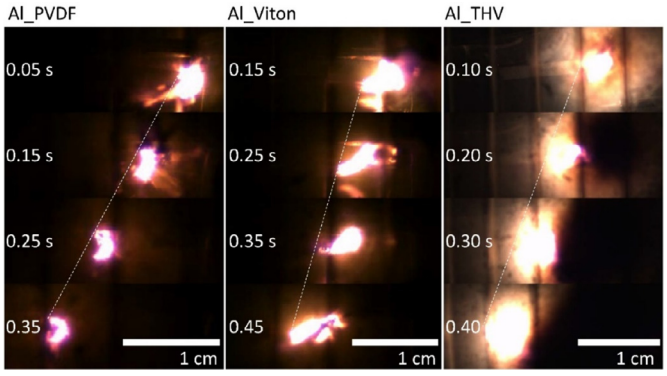

Fig. 3. Burning snapshots of Al_PVDF (a), Al_Viton (b), and Al_THV (c) films (10 layers).

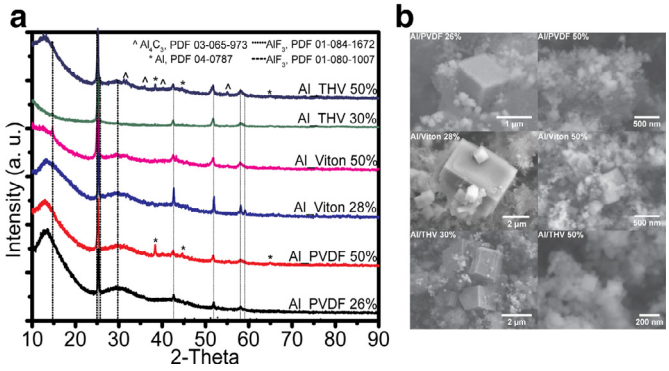

Fig. 5. XRD results and SEM images of combustion products from Al_PVDF, Al_Viton and Al_THV with stoichiometric and 50 wt% Al (10 layers).

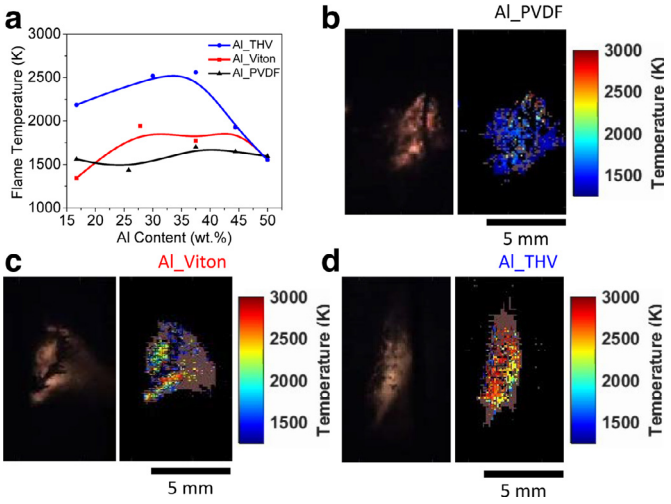

Fig. 4. The average flame temperatures (a) of different films with loading of Al NPs. The typical snapshot and corresponding flame temperature map of stoichiometric Al_PVDF (b, 26 wt% Al), Al_Viton (c, 28 wt%) and Al_THV (d, 30 wt%) films (10 layers). High error points were marked as brown and are excluded from the calculations.

The combustion products were collected and examined by XRD and SEM. As the XRD results (Fig. 5a) show, the major products of all the cases are AlF_3 (and carbon, which is not detectable in XRD but confirmed by EDS as shown in Fig. S3). With increase of Al content, we saw burn rate increase in all the three cases, as well as much smaller AlF_3 product particles forming in the combustion products (Fig. 5b), which is evidence of enhanced heat convection and advection resulting in reduced sintering [17,27]. However, the flame temperature versus Al content peaks slight fuel rich (Fig. 4a), which did not follow the same trend as the burning rate which increases with Al loading (Fig. 2a). For Al/PVDF with 50 wt% Al (fuel rich), excess Al was detected in the combustion products, while for Al/Viton and Al/THV, aside from the Al peaks, a new product of Al_4C_3 was also detected. The Al_4C_3 only being formed in the Al/Viton and Al/THV combustion products may result from reaction between excess Al and C residue. which nominally will require higher temperatures to trigger. In prior work we have actually observed Al_4C_3 when burning Al/PVDF in air because of the higher flame temperature (~1800 K) than in argon atmosphere (~1500 K) [4]. Obviously, the energy density is the highest at stoichiometric consequently, the flame temperature declines rapidly for all the three when it is fuel rich, as shown in Fig. 4a.

To probe the reaction mechanism of aluminum with different fluorine-containing polymers, time-resolved speciation obtained by Time-of-Flight T-Jump Mass Spectrum (T-Jump MS). The normalized and time-resolved HF and CF_3 release of the three composite films were shown in Fig. 6a–c, respectively. Al/PVDF releases the highest amount of HF gas and the least amount of CF_3. The HF release from Al/Viton and Al/THV is roughly the same but much lower than Al/PVDF. This result is consistent with the fact that PVDF has the highest hydrogen content so should yield the highest HF and lowest CF_x, which results in much more H_2 (a side-product from the Al-HF reaction) detected than the other two cases (Fig. 6d). The exothermicity of Al-CF_x (−706 kJ/mol for Al/CF_4) reaction is much higher than Al-HF reaction (−470 kJ/mol). As a result, flame temperatures are Al/THV > Al/Viton > Al/PVDF.

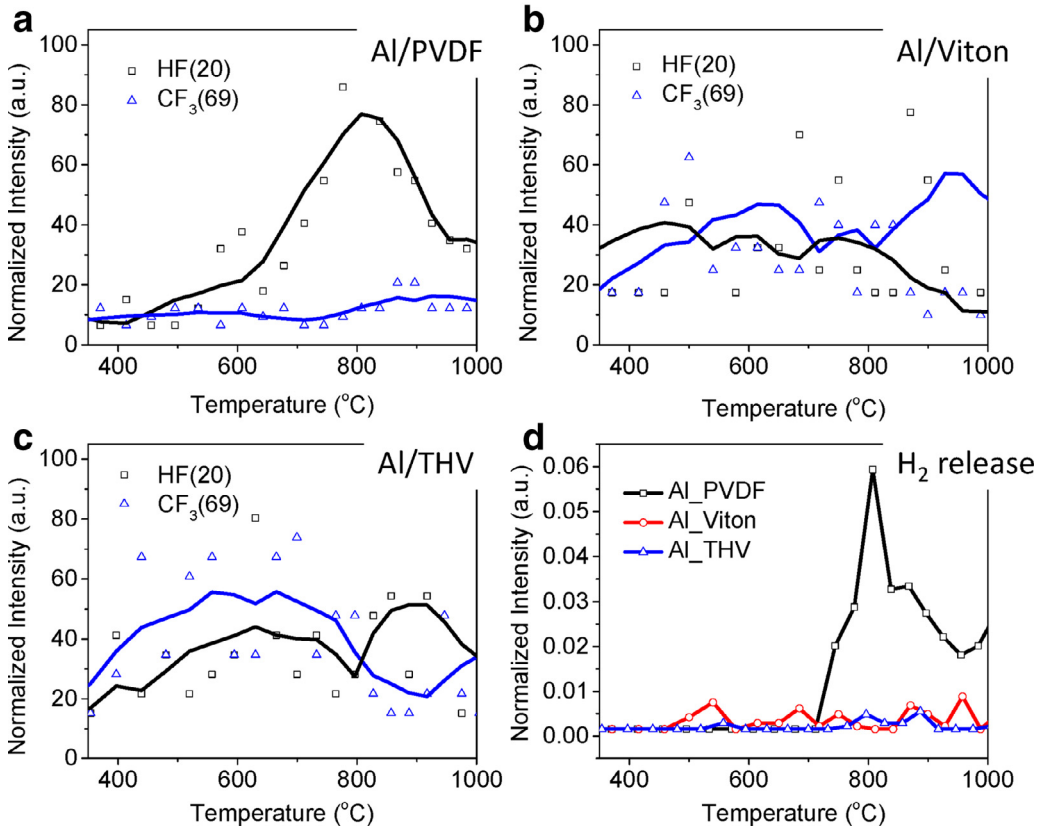

Fig. 6. The HF and CF_3 release of Al_PVDF (a), Al_Viton (b) and Al_THV (c); The H_2 release (d). Note: all the results were obtained from T-Jump Mass Spectrum.

On the other hand, PVDF has by far the lowest ignition temperature (570 °C) because HF release triggers the pre-ignition reaction with the alumina shell [3,28,29] (Fig. S4). Activation energies of the three composites obtained by the Ozawa method from TGA give Al/PVDF ~80–100 kJ/mol which is smaller than that of Al/Viton (100–120 kJ/mol) and Al/THV (110–120 kJ/mol), are presented in Fig. S5 and consistent with PVDF having the lowest ignition temperature.

4. Conclusion

Three soluble fluorine rich polymers of PVDF (59 wt% F), Viton (66 wt% F) and THV (73 wt% F) were incorporated with Al NPs and prepared into free-standing films by direct writing. It is found that tensile elasticity is in the order of Al/PVDF > Al/THV > Al/Viton while the stretchability of Al/Viton is much higher than that of Al/PVDF and Al/THV. Al/PVDF has the highest burn rate compared to the other two. However, the flame temperature is ordered: Al/THV (~2500 K) > Al/Viton (~2000 K) > Al/PVDF (~1500 K). THV releases more CF_x gas than HF while PVDF showed the opposite trend. Al-CF_x produces more heat release Al-HF, thus Al/THV was observed to have the highest flame temperature. However, HF which is strongly produced by PVDF triggers the pre-ignition of Al and reducing its ignition temperature significantly and is a possible explanation why Al/PVDF was the fastest burn even though it had the lowest temperature.

Acknowledgments

This work was supported by the AFOSR. We acknowledge the support of the Maryland Nanocenter and its NispLab. The NispLab is supported in part by the NSF as an MRSEC Shared Experimental Facility. Supporting Information is available online from journal website or from the authors.

Supplementary material

Supplementary material associated with this article can be found, in the online version, at doi:10.1016/j.combustflame.2018.12.031.

References

[1] R. Padhye, A.J.A. Aquino, D. Tunega, M.L. Pantoya, Fluorination of an alumina surface: modeling aluminum-fluorine reaction mechanisms, ACS Appl. Mater. Interfaces 9 (2017) 24290–24297.
[2] S.K. Valluri, M. Schoenitz, E. Dreizin, Fluorine-containing oxidizers for metal fuels in energetic formulations, Def. Technol. (2018), doi:10.1016/j.dt.2018.06.001.
[3] H. Wang, J.B. DeLisio, S. Holdren, T. Wu, Y. Yang, J. Hu, M.R. Zachariah, Mesoporous silica spheres incorporated aluminum/poly (vinylidene fluoride) for enhanced burning propellants, Adv. Eng. Mater. 2 (2018) 1700547.
[4] C. Huang, G. Jian, J.B. DeLisio, H. Wang, M.R. Zachariah, Electrospray deposition of energetic polymer nanocomposites with high mass particle loadings: a prelude to 3D printing of rocket motors, Adv. Eng. Mater. 1 (2015) 95–101.
[5] X. Hu, J.B. DeLisio, X. Li, W. Zhou, M.R. Zachariah, Direct deposit of highly reactive $Bi(IO_3)_3$-polyvinylidene fluoride biocidal energetic composite and its reactive properties, Adv. Eng. Mater. 19 (2017) 1500532.
[6] T.R. Sippel, S.F. Son, L.J. Groven, Aluminum agglomeration reduction in a composite propellant using tailored Al/PTFE particles, Combust. Flame 1 (2014) 311–321.
[7] L. Glavier, G. Taton, J. Ducéré, V. Baijot, S. Pinon, T. Calais, A. Estève, M. Djafari Rouhani, C. Rossi, Nanoenergetics as pressure generator for nontoxic impact primers: comparison of Al/Bi_2O_3, Al/CuO, Al/MoO_3 nanothermites and Al/PTFE, Combust. Flame 5 (2015) 1813–1820.
[8] W. He, P. Liu, F. Gong, B. Tao, J. Gu, Z. Yang, Q. Yan, Tuning the reactivity of metastable intermixed composite n-Al/PTFE by polydopamine interfacial control, ACS Appl. Mater. Interfaces (2018), doi:10.1021/acsami.8b10197.
[9] F.D. Ruz-Nuglo, L.J. Groven, 3-D printing and development of fluoropolymer based reactive inks, Adv. Eng. Mater. 2 (2018) 1700390.
[10] L. De Barros, A.P.M. Pinheiro, J.D.E. Câmara, K. Iha, Qualification of magnesium/teflon/viton pyrotechnic composition used in rocket motors ignition system, J. Aerosp. Technol. Manag. 2 (2016) 130–136.

[11] J.A. Bencomo, S.T. Iacono, J. McCollum, 3D printing multifunctional fluorinated nanocomposites: tuning electroactivity, rheology and chemical reactivity, J. Mater. Chem. A 6 (2018) 12308–12315.
[12] E. Koch, Metal-fluorocarbon-pyrolants: III. Development and application of magnesium/teflon/viton (MTV), Propellants Explos. Pyrotech. 5 (2002) 262–266.
[13] S.L. Row, L.J. Groven, Smart energetics: sensitization of the aluminum-fluoropolymer reactive system, Adv. Eng. Mater. 2 (2018) 1700409.
[14] J.M. Slocik, R. McKenzie, P.B. Dennis, R.R. Naik, Creation of energetic biothermite inks using ferritin liquid protein, Nat. Commun. 8 (2017) 15156.
[15] J. McCollum, A.M. Morey, S.T. Iacono, Morphological and combustion study of interface effects in aluminum-poly (vinylidene fluoride) composites, Mater. Des. 134 (2017) 64–70.
[16] A.K. Murray, W.A. Novotny, T.J. Fleck, I.E. Gunduz, S.F. Son, G.T.C. Chiu, J.F. Rhoads, Selectively-deposited energetic materials: a feasibility study of the piezoelectric inkjet printing of nanothermites, Addit. Manuf. 22 (2018) 69–74.
[17] K.T. Sullivan, C. Zhu, E.B. Duoss, A.E. Gash, D.B. Kolesky, J.D. Kuntz, J.A. Lewis, C.M. Spadaccini, Controlling material reactivity using architecture, Adv. Mater. 10 (2016) 1934–1939.
[18] M.S. McClain, I.E. Gunduz, S.F. Son, Additive Manufacturing of ammonium perchlorate composite propellant with high solids loadings, Proc. Combust. Inst. (2018), doi:10.1016/j.proci.2018.05.052.
[19] S. Ghosh, S.T. Parker, X. Wang, D.L. Kaplan, J.A. Lewis, Direct-write assembly of microperiodic silk fibroin scaffolds for tissue engineering applications, Adv. Funct. Mater. 13 (2008) 1883–1889.
[20] C. Chang, V.H. Tran, J. Wang, Y. Fuh, L. Lin, Direct-write piezoelectric polymeric nanogenerator with high energy conversion efficiency, Nano Lett. 2 (2010) 726–731.
[21] C. Xu, C. An, Y. He, Y. Zhang, Q. Li, J. Wang, Direct ink writing of DNTF based composite with high performance, Propellants Explos. Pyrotech. 8 (2018) 754–758.
[22] R.J. Jacob, D.J. Kline, M.R. Zachariah, High speed 2-dimensional temperature measurements of nanothermite composites: probing thermal vs. gas generation effects, J. Appl. Phys. 11 (2018) 115902.
[23] L. Zhou, N. Piekiel, S. Chowdhury, M.R. Zachariah, T-jump/time-of-flight mass spectrometry for time-resolved analysis of energetic materials, Rapid Commun. Mass Spectrom. 1 (2009) 194–202.
[24] X. Li, P. Guerieri, W. Zhou, C. Huang, M.R. Zachariah, Direct deposit laminate nanocomposites with enhanced propellent properties, ACS Appl. Mater. Interfaces 17 (2015) 9103–9109.
[25] G.M. Dutro, R.A. Yetter, G.A. Risha, S.F. Son, The effect of stoichiometry on the combustion behavior of a nanoscale Al/MoO_3 thermite, Proc. Combust. Inst. 2 (2009) 1921–1928.
[26] C. Seoul, Y.T. Kim, C.K. Baek, Electrospinning of poly (vinylidene fluoride)/dimethylformamide solutions with carbon nanotubes, J. Polym. Sci. Part B: Polym. Phys. 13 (2003) 1572–1577.
[27] G.C. Egan, M.R. Zachariah, Commentary on the heat transfer mechanisms controlling propagation in nanothermites, Combust. Flame 7 (2015) 2959–2961.
[28] J.B. DeLisio, X. Hu, T. Wu, G.C. Egan, G. Young, M.R. Zachariah, Probing the reaction mechanism of aluminum/poly(vinylidene fluoride) composites, J. Phys. Chem. B 24 (2016) 5534–5542.
[29] H. Wang, R.J. Jacob, J.B. DeLisio, M.R. Zachariah, Assembly and encapsulation of aluminum NP's within AP/NC matrix and their reactive properties, Combust. Flame 180 (2017) 175–183.